IDENTIFICATION OF THEORETICAL SHEAR STRENGTH AND ONSET OF YIELDING IN CUBIC BORON NITRIDES VIA NANOINDENTATION

S. Dub[1], I. Petrusha[1], V. Bushlya[2], G. Tolmacheva[3], A. Andreev[1]

[1]Institute for Superhard Materials, Kiev, Ukraine
[2]Division of Production and Materials Engineering, Lund University, Lund, Sweden
[3]Kharkov Institute of Physics and Technology, Kharkov, Ukraine

sergey-dub@bigmir.net

Abstract: The onset of plasticity in cubic boron nitride (cBN) was studied by nanoindentation with continuous stiffness measurement (CSM) option. CSM option allows us to observe elastic-plastic transition in the contact and to measure the yield strength of cBN at nanoscale. In single crystals with low dislocations density sharp elastic-plastic transition (pop-in) was observed as a result of homogeneous dislocations nucleation at shear stress close to theoretical shear strength ($G/2\pi$). For near nanocrystalline cBN sample the smooth elastic-plastic transition was observed as a result of propagation of already existing dislocations in the region of contact.

Keywords: cBN, nanoindentation, elasto-plastic transition, theoretical shear strength.

1. INTRODUCTION

Ya. Frencel in 1926 has shown that the shear stress which is needed for the initiation of plasticity in ideal crystals is equal to $G/2\pi$, where G is shear modulus (Kelly, 1973). This stress is usually referred to as the theoretical shear stress. Theoretical shear stress is by several orders higher than the yield strength of real metals. Such discrepancy between the yield strength for ideal and real crystals is caused by the lattice defects (primarily by dislocations) which make the onset of plasticity easier.

For a long time experimental estimations of theoretical shear strength were possible by testing whiskers crystals only (Berezhkova, 1969). The tests of metallic single crystal whiskers have shown that the actual values of the theoretical shear strength are approximately equal to $G/(10–15)$ (Kelly, 1973). Recently FIB technique was used to obtain the sub-microns samples (Bei *et al.*, 2007, Nadgorny *et al.*, 2008, Dehm, 2009). But all the above mentioned techniques allow us to conduct tests on the plastic materials only. The brittle materials will rupture during the test before the onset of plasticity occurs in the sample. There is another approach – to decrease not sample size, but the size of deformed region, for example, by nanoindentation. During nanoindentation majority of hard and superhard non-metallic materials deform elastoplasticaly. This allows characterizing both elastic and plastic properties of brittle materials. Moreover, in nanoindentation it is easy to create situation when the contact size in single crystal is much less than the average distance between dislocations. In this case a sharp discontinuity (pop-in) is observed on the loading curve due to a homogeneous dislocation nucleation in previously dislocation-free volume under the contact. Such tests give the possibility to make experimental estimation of the theoretical shear stress and ultimate hardness even for brittle materials (Michalske and Houston, 1998, Biener *et al.*, 2007, Dub *et. al.*, 2013).

There are only several publications on studying the mechanical properties of cBN single crystals by nanoindentation (Goken *et al.*, 2001, Zerr *et al.*, 2002), in which the pop-in in cBN single crystal was observed and critical shear stress for onset of plasticity was estimated. The onset of plasticity wasn't studied on nanocrystalline cBN samples.

The goal of the present work was to study the initiation of plasticity during nanoindentation in cBN samples with low (single crystal) and high (near nanocrystalline) dislocations density.

2. EXPERIMENTAL

2.1. Materials and methods

cBN single-crystals were synthesized in the belt-type apparatus with the standard assembly of a high pressure cell (HPC). The process of spontaneous nucleation and the crystal grows were realized in the B-N-Li growth system at pressure 7 GPa and temperature 1800-1900 ºC during 17 hours. The syntesis yielded crystals up to 2.6 mm in size and with varying degree of morphological perfection – even up to polyhedral fullface shapes. The habit of single crystals always included mirror-smooth faces, which correspond to close-packed (111) planes, that were eventually tested via nanoindentation (Fig. 1).

Polycrystalline cBN was synthesized at pressure 8 GPa and temperature ≈ 2250 °C (duration of the cycle 60 s) from high-purity graphite-like quasi-crystalline BN bulk precursor (qcgBN) with a density of about 2 g/cm^3 grown by a CVD method. A toroid type high pressure apparatus (HPTA) and a special HPC assembly were used for the synthesis of the polycrystalline cBN samples which had the disk shape of 12 mm in diameter and approx. 1.4 mm in thickness. Prior to the analysis, they were planar ground to the thickness of 1 mm and subsequently polished with diamond suspension of 9 μm and 1 μm, followed by super-finishing with 40 nm SiO_2 colloidal solution. Extensive duration of the super-finishing (> 1.5 hour) and low process pressure (0.02 MPa) were used to ensure minimal mechanical damage to the material due to grinding and polishing.

2.2. Characterization techniques

Two ultra-high resolution scanning electron microscopes, dual beam FEI Nova NanoLab 600 and Hitachi SU8010 Cold Field Emission SEM, were used for microscopy on poly- and single-crystal cBN respectively. Poor electrical conductivity of the high-purity polycrystalline cBN leads to charging effects during electron microscopy. Carbon coating of the samples was performed prior the SEM inspection, in order to avoid the charging. The coating was then locally pilled-off in the spots of interest.

The mechanical properties of cBN samples were studied by nanoindentation using a Nano Indenter-G200 system (Agilent Technologies) equipped with a continuous stiffness measurement (CSM) option. This option offers a continuous measurement of the contact stiffness via a superimposed alternating current signal during loading, which in turn provides a continuous measurement of the elastic modulus E and hardness H as function of the indenter displacement during a single loading segment (Hay *et al.*, 2010). Ten indentations were made on each sample. A diamond Berkovich tip with some tip blunting was used. AFM measurements of the tip shape have been made, and the results showed that the Berkovich indenter tip can be described as a sphere with an effective radius R of 230 nm when the contact depth is less than 35 nm. Load (P) and displacement (h) were continuously recorded up to a maximum displacement of 200 nm at a constant indentation strain rate of 0.05 s^{-1}.

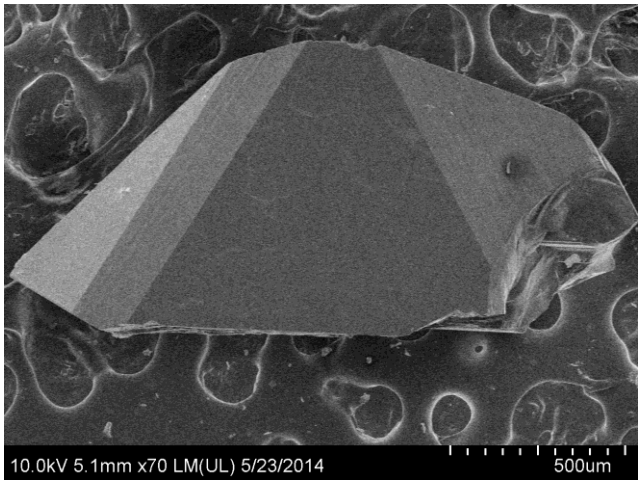

Fig. 1. SEM image of cBN single crystal synthesized at 7 GPa and 1800–1900 °C and containing the habit face {111}.

3. RESULTS AND DISCUSSSIONS

3.1. Scanning electron microscopy

The density of the obtained near-nanocrystalline material reaches ≈ 3.476 g/cm^3 at the end of the qcgBN → cBN solid-solid transformation, which corresponds to the porosity of the material ≈ 0.46 %. The results of the XRD and SEM analysis provide evidence that, with respect to the grain size in the material microstructure, the obtained polycrystalline cBN can be classified as near-nanocrystalline because the grain size is predominantly around 100 nm with fewer grains up to 400 nm. However all grains contain lamellar {111} nanotwins of various thicknesses ranging from 10 to 60 nm (Fig. 2). The probable mechanism of the solid-solid transformation lays in the realization of the following chain of transformations qcgBN→chBN→wBN→cBN, which corresponds to the principle of alternative metastable behavior (Ostwald step rule). Ordering of the qcgBN structure with the formation of crystalline hexagonal BN (chBN) in the p-T zone of cBN stability has been frequently observed (Nikishina M. V. *et al.*, 2009) on the stages of incomplete transformation. This process facilitates the formation of metastable wurtzite BN (wBN) as a consequence of martensite transformation of the ordered structure of chBN. The structure of the being formed wBN, unstable under high temperatures, easily transforms to the thermodynamically stable cBN structure via cooperative mechanisms of stacking faults propagation and twinning (Britun V. F. *et al.*, 2000), thus explaining the observed high density of lamellar {111} nanotwins in the structure of polycrystalline cBN.

According to the analysis of the broadening of XRD diffraction peaks, the lattice strain caused by the microstructural defects in the cBN lattice, by impurity atoms, etc. was estimated to be on the level of e = (4.7–7.6)·10^{-4}. Lattice parameter (Rietveld method) equals a = 0.36165–0.36171 nm, which is significantly higher than the standard value of a = 0.36158 nm (ICDD PDF-2, PDF-card 35-1365).

3.2. Nanoindentation

(111) cBN single crystals. Typical load-displacement curve of a Berkovich indenter for (111) cBN single crystal at a maximum load of 35 mN is presented in Fig. 3. It can be seen from this figure that an abrupt increase in the displacement (pop-in) by 11 nm at a displacement of about 91 nm occurs for a time shorter than 0.17 s. After the unloading of the indenter to zero, one can observe a residual indentation, which indicates that, at a load of 35 mN, plastic deformation takes place in the contact. Critical load P_c for pop-in formation varies in the range from 3.6 to 10.3 mN. The mean value of P_c is equal to 7.9 ± 1.9 mN. The loading cycle is completely reversible during unloading if the test was performed at load $P < P_c$. So, it follows that the pop-in in the initial part of the loading curve corresponds to transition from elastic to elastic-plastic deformation in the contact and that the loading curve before pop-in is a clearly pronounced portion of the elastic deformation in the contact.

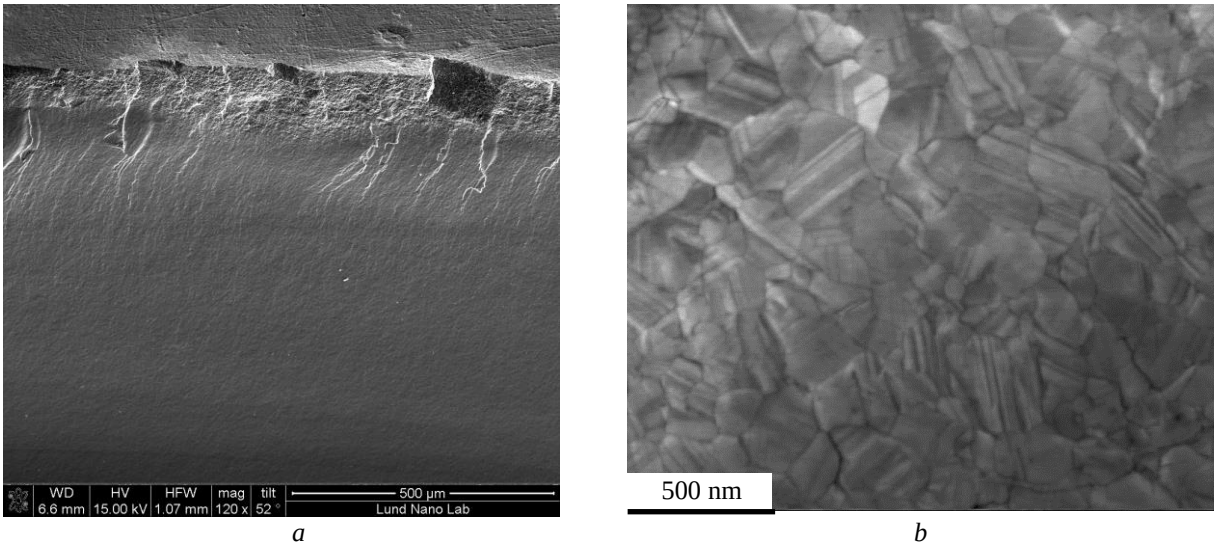

a *b*

Fig. 2. SEM images of a fracture surface (a) and a typical microstructure (b) of near-nanocrystalline cBN synthesized at 8 GPa and 2300 °C from CVD graphite-like BN precursor.

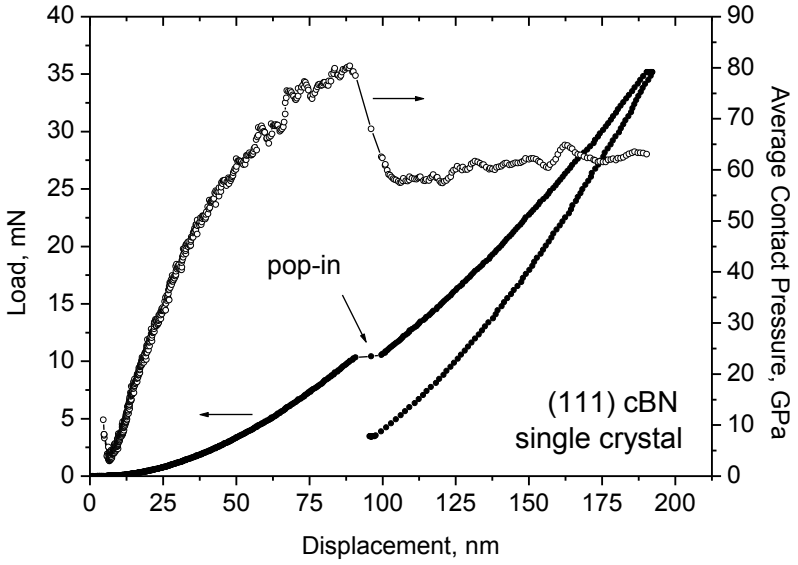

Fig. 3. Nanoindentation tests performed on a cBN (111) single crystal with low dislocation density: load – displacement *P-h* curve with a pronounced discontinuity (pop-in) marking the onset of plasticity, and average contact pressure ACP versus displacement *h*.

The dependence of ACP on the displacement for the (111) cBN single crystal according to the data obtained using the CSM attachment is also shown in Fig. 3. It is seen that ACP reaches the maximum before the pop-in formation in the load–displacement curve. The average value of ACP before pop-in formation ($P = P_c$) for (111) cBN single crystal is 72.4 ± 5.9 GPa (Table 1), upper boundary being 80.6 GPa. After pop-in formation, the ACP decreases to 62 GPa for a period shorter than 1/3 s.

Table 1. Elastic modulus, hardness and critical shear stress for yielding in cBN with low (single crystal) and high (near nanocrystalline cBN sample) dislocations density. Test results for aluminium and sapphire single crystals are also given for comparision.

Sample	Elastic modulus *E*, GPa	Hardness *H*, GPa	Critical shear stress for yielding τ_c, GPa
(111) Al, 99,99 %	72	0.36	2.1 (*G*/12)
(0001) sapphire	470	27.8	23.8 (*G*/7.4)
(111) cBN single crystal	960 ± 27	61.8 ± 1.4	37.5 ± 2.7 (*G*/10)
Near-nanocrystalline cBN	967 ± 34	69.0 ± 2.3	18.7 ± 2.1 (*G*/18)

To analyze the initial elastic section, one may use the contact elasticity theory, whose fundamentals were laid by Hertz more than 100 years ago. According to the atomic force microscopy data, the tip of the Berkovich pyramidal indenter used in testing at the depths ranging from 0 to 35 nm is of a spherical shape with a radius of ~ 230 nm. The maximum shear stresses in the contact for spherical indenter are (Johnson, 1987)

$$\tau_{\max} = \frac{1}{2}|\delta_1 - \delta_3|, \qquad (1)$$

where σ_1 and σ_3 are the principal stresses. The τ_{max} attains the highest value τ_c directly under the indent center ($r = 0$) at a distance of 0.48 indent radius *a* under the sample surface (Johnson, 1987):

$$\tau_c = [0{,}61 - 0{,}23(1 + \nu)]p_{max} \approx 0{,}47p_{mean}, \qquad (2)$$

where p_{mean} is the ACP in the case of the elastic contact of a rigid sphere with a flat surface. As it was already mentioned, the upper boundary of the ACP before the pop-in formation is 80.6 GPa. From Eq. (2) we obtain that the critical shear stresses τ_c at $P = P_c$ for a (111) cBN single crystal is 37.5 GPa (~G/10).

Theoretical shear strength τ_{th} of cBN is equal to 59 GPa ($G/2\pi$), and theoretical (elastic) hardenss ~ 129 GPa ($2.2\tau_{th}$). So, the shear stress in the region of contact before the pop-in formation is approaching the theoretical shear strength just as ACP approaches the theoretical hardness. Indent size in single crystals with low dislocation dencity at h < 100 nm became much less then the average distance between dislocations. In this case there is a high probability that the dislocations (carriers of plastic deformation) are absent in the contact region. As the results, the applied shear stress at the contact grows during the loading but the plastic deformation doesn't begin. Only at the load P_c, at which critical shear stress is close to theretical strength, homogeneous nucleation of the first dislocation loop and its subsequent avalanche multiplication occurs.

The hardness drops to 62 GPa after pop-in formation. It is the hardness of cBN when dislocations in the contact region already exist. Upper boundary of ACP before the pop-in formation (80.6 GPa) gives the experimental estimate of the highest possible hardness for (111) cBN single crystal. Its value would be as high, but for the existing lattice defects (first of all, dislocations), which make the beginning of the plastic flow in crystals easier. Therefore, by suppressing the dislocation propagation, e.g., by forming a nanocrystalline structure, one can increase the cBN hardness up to 81 GPa.

Near nanocrystalline cBN. Nanoindentation test results for near nanocrystalline cBN are given in the Table 1. It can be seen that the hardness is equal to 69 GPa, elastic modulus – 967 GPa. Increase in the hardness, as compared to (111) cBN single crystal, is caused by high density of structural defects (grains boundaries) in near nanocrystalline cBN. Usually, the elastic modulus of nanocrystalline materials is lower than that of single crystal due to a large portion of noncoherent gain boundaries and triple joints in the sample volume. The formation of near nanocrystalline structure with pure (no sintering aids were used) and perfect grain boundaries of recrystallization origin allows us to prevent the drop of elastic modulus for the sample studied.

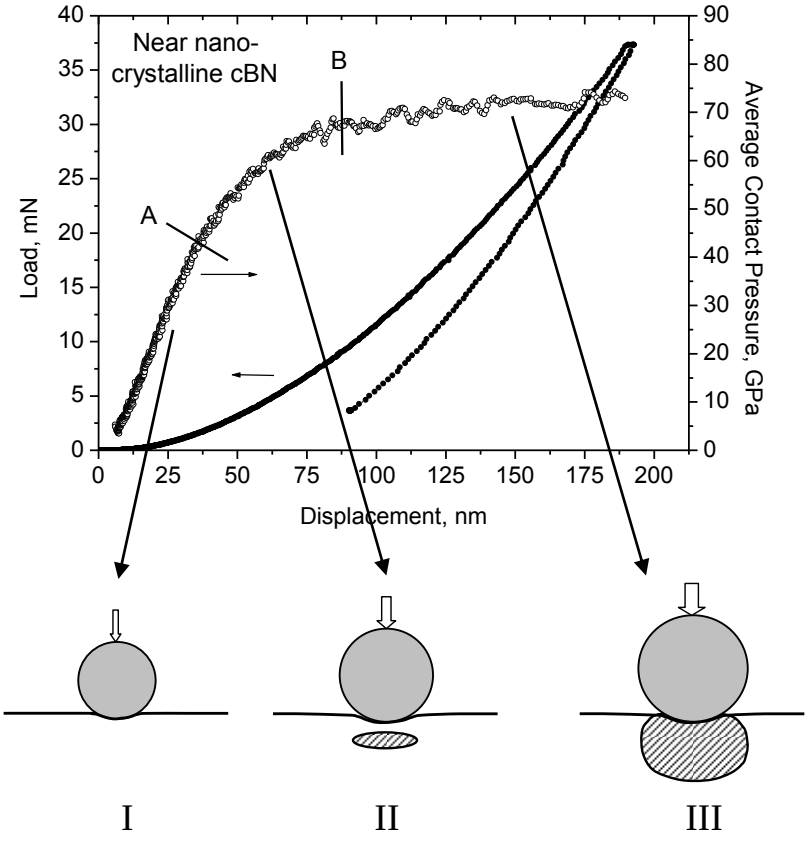

Fig. 4. Load-displacement curve and ACP versus h for near nanocrystalline cBN sample. Regimes of deformation in the contact: I – elastic, II – constrained plastic deformation, III – full plasticity.

Typical load-displacement curve for near nanocrystalline cBN sample is given on Fig. 4. The displacement of the indenter increases monotonously with the increasing indentation load. In the case of near nanocrystalline cBN, even at the depth of contact about 20 – 30 nm, the average distance between dislocation was much less if compared to the contact size. Therefore, in near nanocrystalline cBN, the onset of plasticity is caused by the propagation and multiplication of already existing dislocations without the formation of pop-in.

Fig. 4 shows also the dependence of the average contact pressure (ACP) on the displacement. At first, the ACP increases in direct proportion to the displacement (region I), then ACP continues to increase with the indent depth, but not as quickly as at the beginning (region II). After point B (h = 88 nm) the ACP does not virtually change (region III). A similar dependence of ACP on displacement was earlier observed by D. Tabor (Tabor, 1951) in penetration of a spherical indenter into a prior plastically deformed steel sample. D. Tabor explained the observed trend of the ACP dependence on the displacement by a change of the regimes of the deformations in a contact. According to D. Tabor, only elastic deformation occurs in the contact (see Fig. 1, I) in the first region. At point *A*, the applied shear stress under the imprint achieves the yield strength and a zone of constrained plastic deformation forms, which is surrounded by elastically deformed material (see Fig. 4, II). Upon the further growth of the load, a size of the zone of constrained plastic deformation increases and at point *B* it reaches the sample surface. At this moment a regime of full plasticity in the contact starts (see Fig. 4, III). According to Fig. 4 the onset of plasticity in near nanocrystalline cBN occurs at ACP = 41 GPa (point *A*). Using Eq. (2) we obtain that for near nanocrystalline cBN τ_c for initiation of plasticity is equal to 18.7 GPa (G/18)).

4. CONCLUSIONS

In summary, the experimental estimate of the theoretical shear strength of cBN was obtained using nanoindentation with CSM option. The experimental estimates are in good agreement with the theoretical one (37.5 and 59 GPa, respectively). It has been shown that dislocations in cBN decrease yield strength at a nanoscale. On the other hand, dislocations association (grain boundary) and nano-twinning substantially increase cBN hardness on the stage of full plasticity in the contact.

REFERENCES

Bei H., S. Shim, E. P. George, M. K. Miller, E. G. Herbert and G. M. Pharr (2007). Compressive strengths of molybdenum alloy micro-pillars prepared using a new technique. *Scripta Mater.*, Vol. 57, pp. 397–400.

Berezhkova G. V. (1969). *Needle –like crystals*. Nauka, Moscow.

Biener M. M., J. Biener, A. M. Hodge and A. V. Hamza (2007). Dislocation nucleation in bcc Ta single crystals studied by nanoindentation . *Phys. Rev. B.* Vol. 76, art. 165422.

Britun V. F., A. V. Kurdyumov, I.A. Petrusha (2000). The rBN-hBN-wBN-cBN crystal-oriented transformations in pyrolytic BN. *J. Superhard Mater.*, Vol. 22, No 2, pp. 3-7.

Dehm G. (2009). Miniaturized single-crystalline fcc metals deformed in tension: new insights in size-dependent plasticity. *Progress Mater. Sci.*, Vol. 54, pp. 664–688.

Dub S. N., P. I. Loboda, Yu. I. Bogomol, G. N. Tolmachova and V. N. Tkach (2013). Mechanical properties of HfB_2 whiskers. *J. Superhard Mater.*, No. 4, pp. 51–62.

Goken, M. and M. Kempf (2001). Pop-ins in nanoindentations – the initial yield point. *Z. Metallkd.*, Vol. 92, pp. 1061-1067.

Hay J., P. Agee and E. Herbert (2010). Continuous stiffness measurement during instrumented indentation testing . *Experimental Techniques,* No. 3, pp. 86-94.

Johnson K. (1989). *Contact mechanic*. Mir, Moscow.

Kelly A. (1973). *Strong solids*. Clarendon Press, Oxford.

Michalske T. A. and J. E. Houston (1998). Dislocation nucleation at nano-scale mechanical contacts. *Acta Mater.*, Vol. 46, pp. 391–396.

Nadgorny E. M., D. M. Dimiduk and M. D. Uchic (2008). Size effects in LiF micron-scale single crystals of low dislocation density. *J. Mater. Res.*, Vol. 23, pp. 2829–2835.

Nikishina M. V., P. P. Itsenko (2009). Stability of the nanostructure of pyrolytic BN under thermobaric influence. *Nanosystems, nanomaterials, nanotechnologies*, Vol. 7, No 2, pp. 505–516.

Tabor D. (1951). *Hardness of metals*. Clarendon Press, Oxford.

Zerr, A., M. Kempf, M. Schwarz, E. Kroke, M. Göken and R. Riedel (2002). Elastic moduli and hardness of cubic silicon nitride. *J. Am. Ceram. Soc*. Vol. 85, pp. 86-90.